SF2A 2025
A. Siebert, K. Baillié, M. Béthermin, F. Cantalloube, E. Josselin, N. Lagarde, J. Malzac, J. Richard, L. Selliez, O. Venot (eds)

MAGNETIC FIELDS OF EMBEDDED PROTOSTARS: A SPIROU INVESTIGATION

L. Drouglazet[1], E. Alecian[1], C. Dougados[1], G. Duchêne[1,2], P. Cristofari[3], A. Sousa[1], H. Nowacki[4], K. Perraut[1] and J. Bouvier[1]

Abstract. Magnetism plays a fundamental role in the early evolution of stars, regulating star-disk interactions and angular momentum transfer. While magnetic fields have been extensively studied in Class II objects, their properties during the embedded protostellar stage remain poorly constrained. SPIRou, the near-infrared spectropolarimeter at the Canada-France-Hawaii Telescope (CFHT), provides a powerful tool to probe the magnetic properties of young stellar objects. Within the PROMETHEE (Protostellar Magnetism: Heritage vs Evolution) project, we obtained spectropolarimetric observations of Class I and Flat-Spectrum (FS) protostars, allowing us to detect and characterize their magnetic fields. These sources are expected to host strong magnetic fields generated by dynamo processes in their fully convective interiors. By analyzing the polarized spectra of our sample using the Least-Squares Deconvolution (LSD) technique, we extract Zeeman signatures that reveal the presence and structure of magnetic fields in these objects. From these profiles, we derive the first measurements of large-scale magnetic field strengths in Class I and FS protostars. We present here the first results from a sample of 18 SPIRou targets, aiming at characterizing large-scale magnetic fields.

Keywords: Star formation, magnetic field, protostars, stellar activity, spectropolarimetry

1 Introduction

Class I objects are young stellar sources still deeply embedded within their envelopes of gas and dust (Lada 1987). The preceding stage, Class 0, corresponds to the earliest phase of star formation, following the collapse of the prestellar core and the formation of the Larson core (Larson 1969; Andre et al. 1993). Flat-Spectrum (FS) objects are thought to represent an intermediate evolutionary stage, transitioning from Class I to Class II protostars (Greene et al. 1994).

During the Class II phase, numerous studies have investigated the role of stellar magnetism in regulating star-disk interaction and accretion processes (Bouvier et al. 2007; Bouvier et al. 2014; Hartmann et al. 2016). The magnetic properties of these young stars are relatively well constrained, with typical average surface field strengths between 1 and 2 kG and their large-scale fields are generally characterized by a dominant poloidal and axisymmetric topology, consistent with the presence of dynamo-generated magnetism in fully convective interiors (Zaire et al. 2024).

In contrast, Class I protostars remain challenging to study due to their deeply embedded and highly obscured environments. As a consequence, we still wonder how magnetic fields influence accretion processes in these early-stage stars.

There is evidence that Class I protostars are hot enough to be fully convective (Doppmann et al. 2005), conditions favorable for strong dynamo action and magnetic field generation. Signatures of magnetospheric accretion have already been detected in some Class I objects (Doppmann et al. 2005), suggesting that magnetic regulation of accretion may be active at this stage, as it is for more evolved Class II stars.

Recent advances in near-infrared spectropolarimetry have opened new possibilities for probing the magnetism of embedded protostars. SPIRou is one of them (Donati et al. 2020) and operates in the $YJHK$ bands, allowing

[1] University of Grenoble Alpes, CNRS, IPAG, 38000 Grenoble, France
[2] Astronomy Department, University of California Berkeley, 94720-3411 Berkeley CA USA
[3] Leiden Observatory, Leiden University, PO Box 9513, 2300 RA Leiden, The Netherlands
[4] Université Côte d'Azur, Observatoire de la Côte d'Azur, CNRS, Laboratoire Lagrange, France

observations of protostars largely inaccessible to optical spectropolarimeters. Thanks to its high spectral resolution ($R \approx 70{,}000$) and its sensitivity (reaching $H \sim 9$–10 for a signal-to-noise ratio of 100 in one hour), SPIRou provides unique constraints on the polarization of stellar light, enabling the detection and characterization of large-scale magnetic fields in Class I sources.

A study of 42 Class I and FS protostars was conducted by Flores et al. (2024), focusing on measuring the averaged strength of the total magnetic field using the high-resolution near-infrared echelle spectrograph iSHELL on the IRTF (Hawaii). They reported a median magnetic field strength of about 1.9 kG, comparable to that measured in Class II stars and consistent with earlier results on Class I sources (Johns-Krull et al. 2009). These findings suggest that strong magnetic fields are already in place during the main accretion phase, likely playing a central role in regulating mass inflow and angular momentum removal very early in stellar evolution.

Here we present our investigation and analysis of large-scale magnetic field in a sample of 18 Class I and FS protostars using SPIRou.

2 SPIRou observations

To characterize magnetic fields using the circular polarization signal induced by the Zeeman effect in photospheric lines, we selected a sample of 18 Class I and FS objects located in several nearby star-forming regions: Perseus, Taurus, ρ Ophiuchus, Serpens, Corona Australis, and Cygnus. When available, the spectral types of the observed sources range from G7 to M6, with the majority between K1 and M4. The projected rotational velocities ($v \sin i$), when known, span from 5 to 52 km s^{-1}. These properties are representative of the typical characteristics observed in embedded protostellar objects (White & Hillenbrand 2004; Doppmann et al. 2005).

Fourteen Class I and FS objects were obtained from PI programs allocated over several semesters (PI: E. Alecian). We also included SPIRou Legacy Survey (SLS) data (Cloutier et al. 2018) for a few additional Class I sources: V347 Aur, HL Tau, the first observation of V512 Per in 2020, GY92 214, and GY92 378 (PI: J.-F. Donati).

All observations were reduced using version V0.7.292 of the dedicated APERO pipeline (Cook et al. 2022).

3 Magnetic field analysis

To analyze the magnetic signals within the photospheric lines, spectra must first be normalized to their continuum. For this purpose, we developed a dedicated normalization tool for SPIRou data called `Fantasio`*. The polarized spectra were then extracted with the `spirou-polarimetry` package of Martioli (2020).

The effective temperature ($T_{\rm eff}$) of each star was derived from fits of spectra computed with `ZeeTurbo` (Cristofari et al. 2023), which takes into account the magnetic field. In our sample of 18 sources, one object was excluded because no photospheric lines were identified, and two others were removed due to insufficient signal-to-noise ratios. In the remaining 15 protostars, effective temperatures, $T_{\rm eff}$ range from 3250 K to 4500 K with a median of 3780 K and an uncertainty of 200 K.

The magnetic field analysis was carried out with the Least-Squares Deconvolution (LSD) method (Donati et al. 1997). This multi-line technique combines the signal from many spectral lines simultaneously, thereby significantly increasing the signal-to-noise ratio of the Stokes V profiles and enhancing the detectability of Zeeman signatures. LSD assumes that an observed spectrum can be modeled as the convolution of an intrinsic line profile with a line mask indicating the position, depth, and magnetic sensitivity of the lines. By inverting this process, LSD recovers the average line profile from the observed spectrum. The line masks used in this analysis were generated from the VALD database†, (Piskunov et al. 1995), based on the estimated $T_{\rm eff}$ of each source.

The LSD profiles were then obtained using the `SpecpolFlow` package‡ developed by Folsom et al. (2025). The resulting profiles are the intensity (Stokes I), the circularly polarised (Stokes V), and the null polarisation spectra (N).

A magnetic detection corresponds to a coherent non-zero signal across the width of the line in Stokes V, with no counterpart in the null profile. Figure 1 illustrates both a clear Zeeman detection (V806 Tau) and a non-detection (IRAS 04292+2422 W).

---

*`https://github.com/Lisa2626/Fantasio`

†`https://vald.astro.uu.se/`

‡`https://github.com/folsomcp/specpolFlow`

To assess the robustness of detections, we computed the False Alarm Probability (FAP) following the criteria defined by Donati et al. (1997), using `SpecpolFlow`. A star was considered magnetic if at least one definite detection ($< 10^{-5}$) was obtained in a given observation. Out of the 15 protostars analyzed, six show definite detections, while nine present no detectable magnetic signature.

In addition, we computed the mean longitudinal magnetic field component (B_ℓ), which represents the line-of-sight projection of the stellar magnetic field integrated over the surface. To investigate why some stars exhibit detectable magnetic fields while others do not, we searched for correlations between magnetic detection and some parameters such as effective temperature, signal-to-noise ratio, and rotational velocity. No significant correlations were identified, indicating that these parameters do not introduce observational biases. Figure 2 shows the effective temperature as a function of projected rotational velocity, with symbol sizes scaling with the strength of B_ℓ. We do not observe any link between these two parameters and the detection of magnetic fields. To assess the impact of data quality, we also examined the relation between magnetic field detection and the uncertainty of longitudinal field measurements. Again, no correlation was found, suggesting that noise levels cannot account for the non-detections.

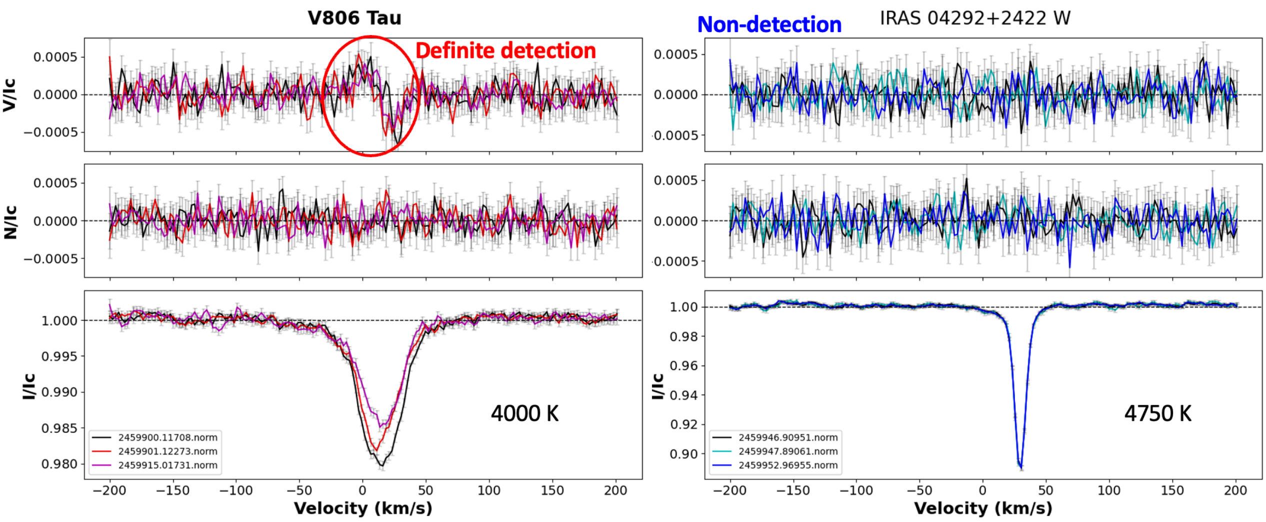

Fig. 1. Left: LSD profiles of V806 Tau. Different colours represent different observations. The Y-axes are I/Ic, N/Ic, and V/Ic, where Ic is the intensity of the stellar continuum. The I profiles show depth variations, due to varying veiling levels. The Stokes V profile displays a clear Zeeman signature, while the N profile remains flat, confirming the astrophysical nature of the detection. **Right:** LSD profiles of IRAS 04292+2422 W, showing no magnetic detection in Stokes V.

4 Conclusions

We report new large scale magnetic field measurements for 15 protostars. Approximately $\sim$40% of the sample exhibit definite magnetic detections according to the FAP criterion, with longitudinal field strengths ranging from -150 to $+262$ G. These values are complementary to those of Flores et al. (2024). Large-scale magnetic field strengths tend to be lower because magnetic components can partially cancel at the stellar surface. One way to directly compare the results would be to also measure the small-scale magnetic field of our sample.

The remaining stars of the sample show no detectable Stokes V signatures, although weak or complex fields may remain hidden below our sensitivity threshold.

Our results demonstrate that Class I and FS protostars can host detectable large-scale magnetic fields with strengths slightly weaker than those typically observed in more evolved objects. This supports the idea that dynamo-driven magnetism and magnetospheric processes are already active during the main accretion phase, potentially shaping star-disk interactions from the earliest stages of stellar evolution. Future work is needed to investigate why magnetic signatures are not detected in all objects, and whether this reflects intrinsic differences in magnetic topology, variability, or observational limitations.

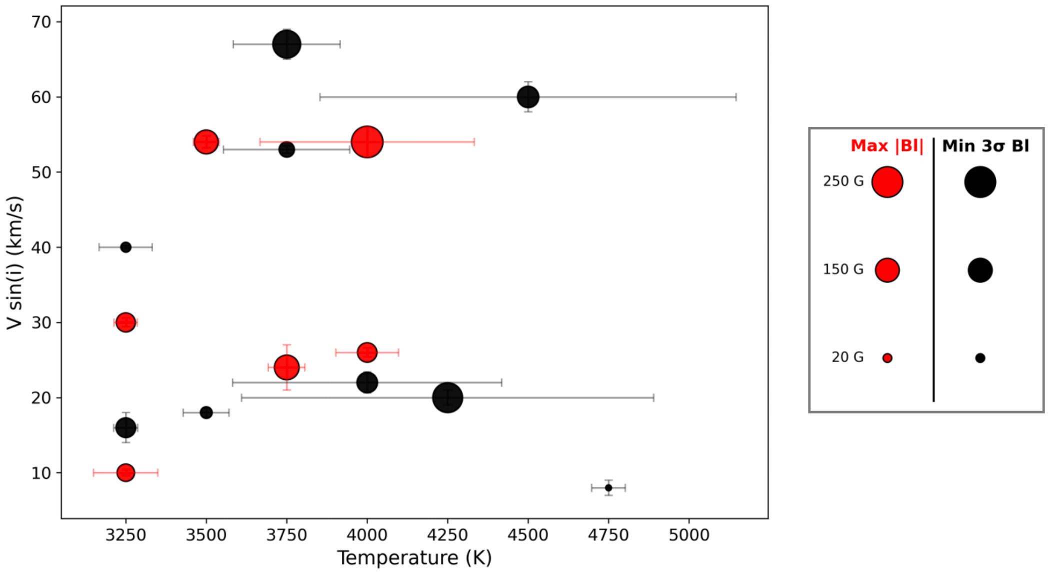

Fig. 2. Projected rotational velocity as a function of the effective temperature. Symbol size is proportional to the maximum absolute value of the longitudinal magnetic field for magnetic stars (red). For non-detections (black), symbol size is proportional to the 3σ upper limits on B_ℓ with their associated uncertainties.

Thank you to the organizers of the SF2A 2025!

References

Andre, P., Ward-Thompson, D., & Barsony, M. 1993, ApJ, 406, 122

Bouvier, J., Alencar, S. H. P., Harries, T. J., Johns-Krull, C. M., & Romanova, M. M. 2007, Protostars and Planets V, 479

Bouvier, J., Matt, S. P., Mohanty, S., et al. 2014, in Protostars and Planets VI, ed. H. Beuther, R. S. Klessen, C. P. Dullemond, & T. Henning, 433–450

Cloutier, R., Artigau, É., Delfosse, X., et al. 2018, AJ, 155, 93

Cook, N. J., Artigau, É., Doyon, R., et al. 2022, PASP, 134, 114509

Cristofari, P. I., Donati, J. F., Folsom, C. P., et al. 2023, MNRAS, 522, 1342

Donati, J. F., Kouach, D., Moutou, C., et al. 2020, MNRAS, 498, 5684

Donati, J. F., Semel, M., Carter, B. D., Rees, D. E., & Collier Cameron, A. 1997, MNRAS, 291, 658

Doppmann, G. W., Greene, T. P., Covey, K. R., & Lada, C. J. 2005, AJ, 130, 1145

Flores, C., Connelley, M. S., Reipurth, B., Boogert, A., & Doppmann, G. 2024, arXiv e-prints, arXiv:2405.12451

Folsom, C. P., Erba, C., Petit, V., et al. 2025, arXiv e-prints, arXiv:2505.18476

Greene, T. P., Wilking, B. A., Andre, P., Young, E. T., & Lada, C. J. 1994, ApJ, 434, 614

Hartmann, L., Herczeg, G., & Calvet, N. 2016, ARA&A, 54, 135

Johns-Krull, C. M., Greene, T. P., Doppmann, G. W., & Covey, K. R. 2009, ApJ, 700, 1440

Lada, C. J. 1987, in IAU Symposium, Vol. 115, Star Forming Regions, ed. M. Peimbert & J. Jugaku, 1

Larson, R. B. 1969, MNRAS, 145, 271

Martioli, E. 2020, SPIRou-Polarimetry: Polarimetry module of the SPIRou Data Reduction Software (DRS), `https://github.com/edermartioli/spirou-polarimetry`, accessed: 2025-07-20

Piskunov, N. E., Kupka, F., Ryabchikova, T. A., Weiss, W. W., & Jeffery, C. S. 1995, Astronomy and Astrophysics Supplement, 112, 525, provided by the SAO/NASA Astrophysics Data System

White, R. J. & Hillenbrand, L. A. 2004, ApJ, 616, 998

Zaire, B., Donati, J. F., Alencar, S. P., et al. 2024, MNRAS, 533, 2893